A nonstorm time enhancement of relativistic electrons in the outer radiation belt

Quintin Schiller,[1,2] Xinlin Li,[1,2] Lauren Blum,[1,2] Weichao Tu,[3] Drew L. Turner,[4] and J. B. Blake[5]

Received 29 October 2013; revised 27 November 2013; accepted 28 November 2013; published 15 January 2014.

[1] Despite the lack of a geomagnetic storm (based on the *Dst* index), relativistic electron fluxes were enhanced over 2.5 orders of magnitude in the outer radiation belt in 13 h on 13–14 January 2013. The unusual enhancement was observed by Magnetic Electron Ion Spectrometer (MagEIS), onboard the Van Allen Probes; Relativistic Electron and Proton Telescope Integrated Little Experiment, onboard the Colorado Student Space Weather Experiment; and Solid State Telescope, onboard Time History of Events and Macroscale Interactions during Substorms (THEMIS). Analyses of MagEIS phase space density (PSD) profiles show a positive outward radial gradient from $4 < L < 5.5$. However, THEMIS observations show a peak in PSD outside of the Van Allen Probes' apogee, which suggest a very interesting scenario: wave-particle interactions causing a PSD peak at $\sim L^* = 5.5$ from where the electrons are then rapidly transported radially inward. This letter demonstrates, for the first time in detail, that geomagnetic storms are not necessary for causing dramatic enhancements in the outer radiation belt. **Citation:** Schiller, Q., X. Li, L. Blum, W. Tu, D. L. Turner, and J. B. Blake (2014), A nonstorm time enhancement of relativistic electrons in the outer radiation belt, *Geophys. Res. Lett.*, *41*, 7–12, doi:10.1002/2013GL058485.

1. Introduction

[2] The relativistic electron population in the outer radiation belt is extremely volatile during periods of enhanced geomagnetic activity. During these times, it is constantly subjected to processes, such as loss, transport, and acceleration, which all compete and blend to affect the net electron population in the outer belt. The result is that geomagnetic storms can deplete, enhance, or cause little effect on the outer radiation belt [*Reeves et al*., 2003]. A detailed understanding of loss, source, and transport is required to fully understand the dynamics of Earth's natural particle accelerator.

[3] Acceleration mechanisms, which replenish the relativistic electron content, can be classified into two broad categories: radial transport and internal acceleration. Radial transport mechanisms can again be broadly classified into two subcategories: radial diffusion and sudden injection, both of which violate the third adiabatic invariant. Radial transport requires an electron source population at high L, such as the plasma sheet in the tail of the magnetosphere [e.g., *Ingraham et al*., 2001]. Radial transport by diffusion in the third adiabatic invariant is a result of incoherent scattering by ULF waves in the Pc4–5 band [e.g., *Tu et al*., 2012]. Sudden injection, which is nondiffusive, can occur from a strong interplanetary shock, for example. Both of these mechanisms are well associated with geomagnetic activity [e.g., *Elkington et al*., 1999; *Li et al*., 2003]. Both also result in a smoothing of the phase space density (PSD) radial profile and thus cannot by themselves create local peaks in PSD.

[4] Local acceleration, on the other hand, is a result of the violation of electrons' first or second adiabatic invariant. This process is also well associated with geomagnetic activity. One local acceleration mechanism is VLF chorus waves, which can resonate with the electrons' gyration period to accelerate them to relativistic energies [e.g., *Meredith et al*., 2003]. Unlike radial transport, this mechanism produces a peak in PSD where the resonant interaction is occurring [e.g., *Chen et al*., 2007; *Reeves et al*., 2013]. Gyroresonant wave-particle interactions are theorized to be a significant contributor to accelerating electrons to relativistic energies [e.g., *Horne and Thorne*, 1998].

[5] Electron acceleration mechanisms in the magnetosphere, and thus enhancements in the outer radiation belt, are strongly correlated with geomagnetic activity. This relation has been recognized for decades, especially in association with the *Dst* index [e.g., *Dessler and Karplus*, 1961]. More recently, *Li et al*. [2001] further substantiate the association by finding a strong correlation between the *Dst* index and SAMPEX 2–6 MeV electron enhancements near geosynchronous orbit (GEO). *Reeves* [1998] investigate electron flux measurements of 0.7 to 7.8 MeV using LANL-GEO spacecraft. Their study, which looks at 43 enhancements from 1992 to 1995, finds that every relativistic electron enhancement in the study is associated with a magnetic storm.

[6] Geomagnetic storms are typically defined as when $Dst < -30$ nT [*Gonzalez et al*., 1999], but sometimes a lower threshold is used. For example, *O'Brien et al*. [2001] do a thorough statistical analysis of electron enhancements of 0.3–1.5 MeV and >2 MeV electrons from LANL GEO from 1992 to 2000. They attempt to correlate electron enhancements with both internal and external drivers and find that long-duration Pc-5 ULF wave activity is an indicator of electron enhancement. However, the study only selects events

[1]Department of Aerospace Engineering Sciences, University of Colorado Boulder, Boulder, Colorado, USA.
[2]Laboratory for Atmospheric and Space Physics, University of Colorado Boulder, Boulder, Colorado, USA.
[3]Space Science and Applications, ISR-1, Los Alamos National Laboratory, Los Alamos, New Mexico, USA.
[4]Department of Earth, Planetary, and Space Sciences, University of California, Los Angeles, California, USA.
[5]Space Sciences Department, Aerospace Corporation, Los Angeles, California, USA.

Corresponding author: Q. Schiller, Department of Aerospace Engineering Sciences, University of Colorado Boulder, Boulder, CO 80303, USA. (quintinschiller@gmail.com)

0094-8276/14/10.1002/2013GL058485

with $Dst < -50$ nT, which omits events with little geomagnetic activity and thus potentially neglects acceleration mechanisms that cause the enhancement of radiation belt electrons during relatively quiet geomagnetic conditions. Events such as the one described in this letter demonstrate that filtering by geomagnetic activity can exclude some significant enhancement events.

[7] Perhaps due to selection criteria, or due to the strong association between electron enhancements and geomagnetic activity, there has not been a detailed reported case of a sudden (<13 h), extreme (>330X) enhancement of electron flux in the outer belt that is not associated with a geomagnetic storm. Some recent studies have begun to allude to the separation between enhancement events and *Dst*; for example, *Borovsky and Denton* [2006] argue that the *Dst* index is a poor indicator of storm properties. *Miyoshi and Kataoka* [2008] use a −50 nT threshold in *Dst* to conclude that magnetic storms are not essential for >2 MeV electron flux enhancements at GEO. *Lyons et al*. [2005] state that >2 MeV electron fluxes at GEO during August to December 2003 increase for every high-velocity solar wind speed event (>500 km/s) regardless of an associated storm. They point out two events with small *Dst* signature and a corresponding relativistic electron enhancement. However, neither event is investigated in detail. Similarly, *Kim et al*. [2006] find two GEO >2 MeV electron enhancement events with $Dst > -30$ nT from 1999 through 2002. With these two events, they also suggest that storm time conditions are not required to create a mega electronvolt electron flux enhancement at GEO.

[8] Expanding on these previous studies, this letter is the first to detail a sudden, extreme relativistic electron enhancement at and inside GEO that occurs during nonstorm time conditions. The enhancement increases flux levels by a factor of >330 in less than 13 h at $L = 5.5$. We employ a unique multipoint measurement configuration to observe the outer radiation belt, which provides unprecedented spatial and temporal coverage and instrument quality. These quality measurements enable a detailed investigation of the timing, energy dependence, and potential causes of the relativistic electron acceleration during this nonstorm enhancement (there are at least two other similar, but less intense, events that are also observed by the Van Allen Probes in its first year). We calculate radial PSD profiles to determine the likely cause of rapid electron acceleration during this nonstorm time event. Additionally, we quantify the relative contribution of concurrent precipitation loss since, ultimately, the enhancement results from energization processes dominating over losses.

2. Data

[9] Electron measurements from the Van Allen Probes mission/RBSP-ECT suite [*Spence et al*., 2013], namely from the Magnetic Electron Ion Spectrometer (MagEIS) instruments [*Blake et al*., 2013], are used for in situ relativistic electron flux and phase space density (PSD) measurements. Spin-averaged fluxes from the MagEIS Medium M75 and High instruments are converted to PSDs for fixed first and second adiabatic invariant for a range of μ centered at 750 (735–765) MeV/G (corresponding to ~550 keV at GEO) and $K < 0.13\ \mathrm{G}^{1/2}R_E$ (mirroring electrons with pitch angles from 90 ± ~35°) via the method described in *Chen et al*. [2006]. Analysis shows that the pitch angle distribution is heavily peaked near the magnetic equator, thus, we can treat the spin-averaged flux measurements as locally mirroring electrons. Background counts due to cosmic rays, solar particles, bremsstrahlung, or electron backscatter have not been removed from the data, but are expected to be small during this event.

[10] Additional electron measurements are analyzed from the Solid State Telescope (SST) instruments onboard the Time History of Events and Macroscale Interactions during Substorms (THEMIS) mission [*Angelopoulos*, 2008]. Flux measurements from the four highest energy channels (from ~400 keV to several MeV) on probes D and E are converted to PSD coordinates for fixed first and second adiabatic invariants $\mu = 750$ MeV/G and $K < 0.01\ \mathrm{G}^{1/2}R_E$ (nearly equatorially mirroring electrons with pitch angles from 90 ± 15°). Details on the THEMIS PSD conversion can be found in *Turner et al*. [2012b]. THEMIS and MagEIS PSDs have not been cross calibrated, so variation in the absolute magnitude is expected. The T89 magnetic field model [*Tsyganenko*, 1989] with real *Kp* input is used for both MasgEIS and THEMIS PSD calculations.

[11] Finally, electron flux measurements are also used from the Colorado Student Space Weather Experiment (CSSWE), a 3U CubeSat in low Earth orbit. These measurements provide insight into the bounce- and drift-loss cones, which cannot currently be resolved from equatorial orbiting measurements like those of the Van Allen Probes or THEMIS. The instrument onboard CSSWE is the Relativistic Electron and Proton Telescope Integrated Little Experiment (REPTile), which measures 6 s directional fluxes of energetic electrons from 0.58 MeV to >3.8 MeV in two differential and one integral channel. Details of the mission and instrument can be found in *Li et al*. [2012, 2013].

[12] Solar wind data and geomagnetic indices are acquired from the OMNI data set. The T89 magnetic field model [*Tsyganenko*, 1989], with real *Kp* inputs, is used in the ONERA IRBEM-LIB toolset for all PSD calculations. The *Dst* index is calculated every hour and available in near-real time. Provisional and final versions of the *Dst* index, which are respectively more accurate than the previous versions, are released within a few years of the real-time *Dst* index. Predicted *Dst*, as seen in Figure 1i, is obtained from the *Temerin and Li* [2002, 2006] model and is available online (http://lasp.colorado.edu/space_weather/dsttemerin/dsttemerin.html). The predicted value has a 0.956 correlation with final *Dst* and is potentially a more accurate representation of final *Dst* than the real-time or provisional indices, as demonstrated in *Temerin and Li* [2002].

3. Detailed Event Analysis

[13] The period of interest terminates an extended quiet period for outer belt electron fluxes beginning around 10 December 2012. Solar wind and geomagnetic parameters are shown in Figure 1, along with electron flux measurements from the Van Allen Probes A and B MagEIS instruments (MagEIS A + B) 0.6 MeV channel and the REPTile 0.58–1.63 MeV channel. A weak high-speed stream (HSS) with maximum velocity reaching almost 600 km/s can be seen to arrive late on 13 January 2013. For this event, the real-time and predicted *Dst* indices peak at −30 nT and −27 nT, respectively, and the *Kp* index peaks at 4−. Additionally, the HSS lacks a strong stream-interface (SI) region, which can be seen by the modest increase to 10 #/cc in the solar wind density and increase of just 1 nPa in solar wind pressure.

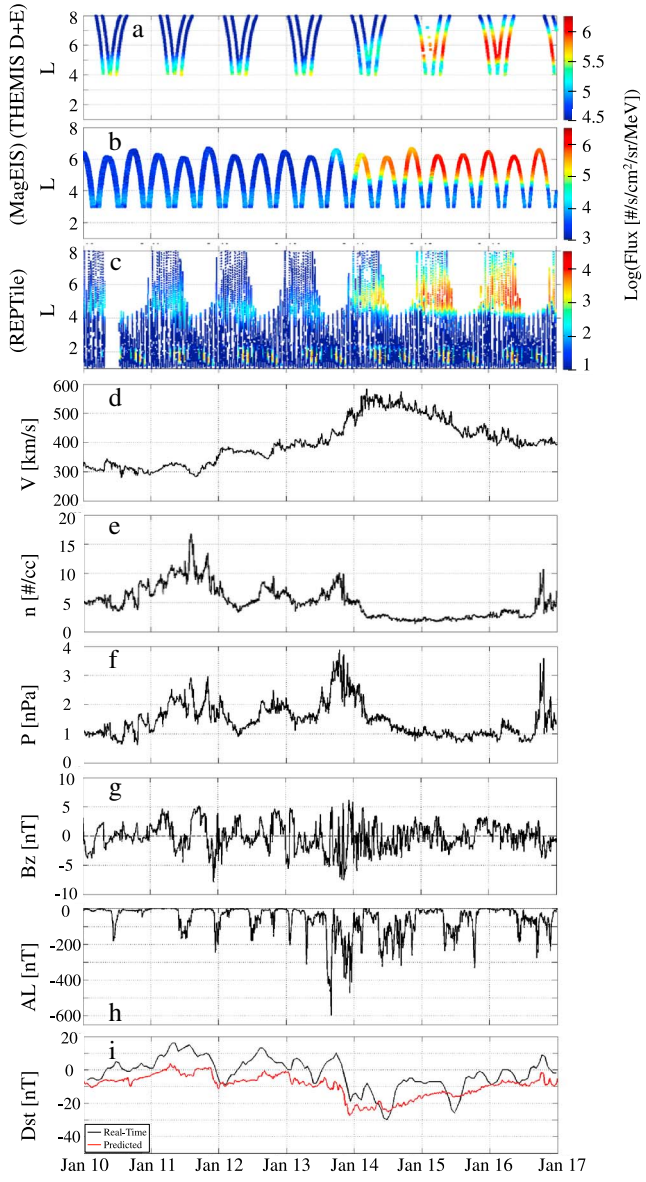

Figure 1. Electron flux measurements and solar wind parameters during the January 2013 enhancement event. (a) Flux measured by THEMIS probes D and E 0.65 MeV electron channel. (b) Flux measured by the MagEIS ~0.6 MeV electron channel on both Van Allen Probes A and B. THEMIS measurements below $L = 4$ and MagEIS measurements below $L = 3$ are not included due to electron and proton contamination, respectively. (c) Electron flux measurements from the CSSWE CubeSat's 0.58–1.63 MeV channel. (d–g) Solar wind parameters, with (h and i) geomagnetic indices *AL* and *Dst*. The predicted *Dst* index (red) can be a more accurate representation of the final *Dst* index than the real-time *Dst* index [*Temerin and Li*, 2002, 2006].

For comparison, in a statistical analysis of 32 CIR driven events from 1994 to 2002, *Denton et al*. [2006] find the mean peak *Dst* and *Kp* indices to be ~−59 nT and 5−, respectively. *Morley et al*. [2010] examine 67 SIs from 2005 through 2008 and find the median density to be ~20 #/cc, with 10 #/cc falling well outside of the interquartile range. There is isolated substorm activity concurrent with the HSS impact, as indicated in the *AL* index.

[14] An enhancement of relativistic electrons is observed by MagEIS near $L \sim 6$ on its inbound orbit during the second half of 13 January nearly simultaneous with the arrival of the HSS, as seen in Figure 1b. On the subsequent orbit, near 14 January 00:00, the enhancement is seen inside of $L = 5$. REPTile observations also measure the enhancement inside of $L = 5$ just prior to 14 January 00:00. At $L = 5.5$, the MagEIS 0.58 MeV flux is enhanced 336 times in under 13 h, from the outbound orbit around 13 January 15:30 to the inbound orbit near 14 January 04:30. The sudden electron enhancement can be seen on all MagEIS channels up to 1.3 MeV, as well as REPTile E1 channel: 0.58 to 1.63 MeV, as seen in Figure 2.

[15] The immediate and rapid enhancement is seen in neither MagEIS nor REPTile energy channels above 1.3 MeV, although these energies are gradually enhanced over the ensuing days. Some potential explanations are that the acceleration mechanism has upper energy threshold, beyond which the electrons are not as effectively accelerated; that the acceleration mechanism is not active for long enough to accelerate the electrons to higher energies; or that the inward radial transport from $L \sim 6.5$, which is likely the cause of the relativistic electron flux enhancement measured by MagEIS, occurs more rapidly for the lower energy electrons. It is of note that in both Figures 1 and 2 the measured particle flux is 1 to 2 orders of magnitude lower as observed by REPTile than MagEIS. Since REPTile is in a low Earth orbit, as compared to the geotransfer-like orbit of MagEIS, it measures only the tail ends of the pitch angle distribution, corresponding to $< \sim 6°$ equatorial pitch angle at $L = 6$.

[16] The phase space density (PSD) profiles for $\mu \sim 750$ MeV/G and $K < 0.13\ \mathrm{G}^{1/2}\ R_E$, as measured by MagEIS and depicted in Figure 3 (top), show a positive radial gradient through $L^* = 5.5$ during the enhancement (as the Van Allen Probes' apogees are at ~5.8 R_E, they cannot measure much

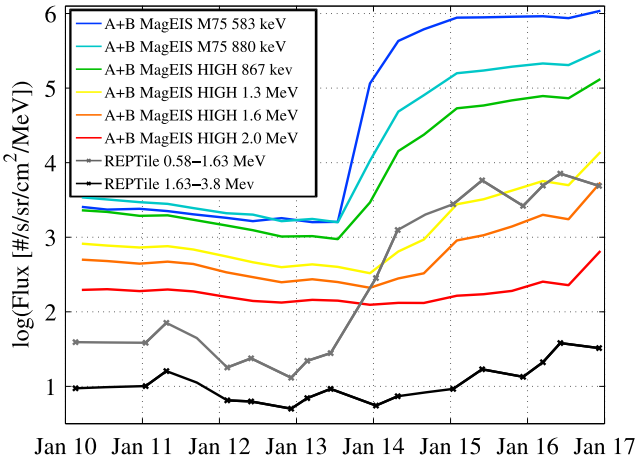

Figure 2. Nine hour flux averages for various MagEIS and CSSWE energy channels. The averages are taken at $L = 5.5$. The sudden and intense electron enhancement late on 13 January is most pronounced at energies from ~0.6–0.9 MeV. The higher-energy electrons are enhanced more gradually over the subsequent few days. Discrepancies between MagEIS M75 and HIGH instruments are expected; MagEIS HIGH channel thresholds were changed after this period to improve agreement between the instruments.

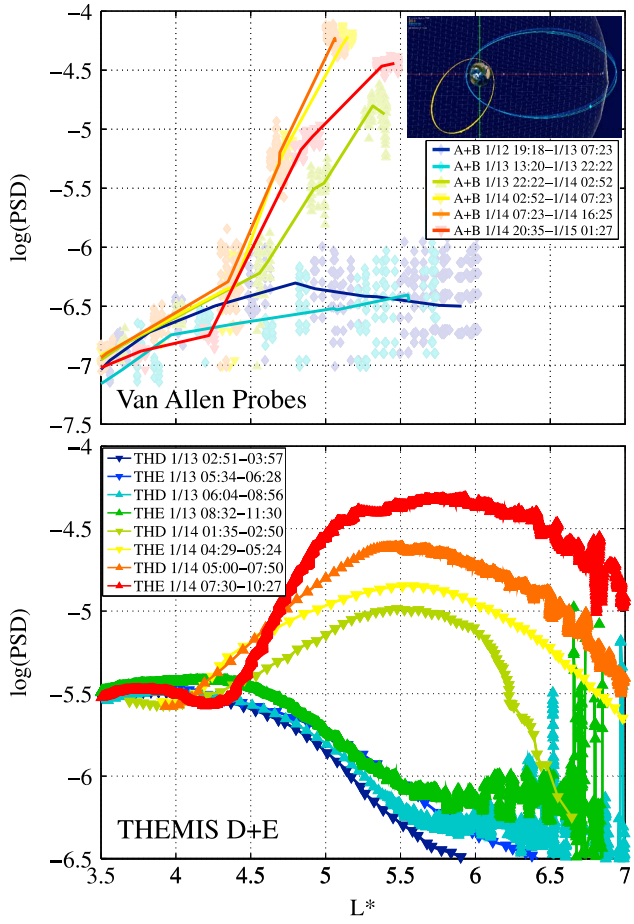

Figure 3. Phase space density (PSD) gradients for constant μ and K during the 12–15 January 2013, enhancement event. Cool colors correspond to earlier times in the period and warmer colors to later times in the period. Upward triangles indicate outbound passes, downward triangles inbound passes, and diamonds from both inbound and outbound portions of the orbit. (top) PSD radial gradients from MagEIS Medium M75 and HIGH instruments on both Van Allen Probe spacecraft for $\mu = 735$–765 MeV/G and $K < 0.13\,\mathrm{G}^{1/2}R_E$. The profile is shown with the opaque line and the data points used to calculate the profile are shown in transparent triangles/diamonds. These radial profiles evolve from relatively flat to positive outward gradient. The inset depicts the orbits of the Van Allen Probes (yellow and orange) and THEMIS D and E (cyan and blue) in the GSE x–y plane, with the Sun to the right. (bottom) PSD radial distributions from THEMIS D and E spacecraft for $\mu = 750$ MeV/G and $K < 0.01\,\mathrm{G}^{1/2}R_E$. Passes after 14 January 01:35 show peaks in PSD between $5 < L^* < 6$. Noise at higher L is due to poor statistics in the counts-to-PSD conversion. THEMIS and MagEIS have not been intercalibrated for this study, which can result in absolute and scaling differences. Additionally, THEMIS PSD measurements below $L = 5$ are susceptible to contamination from higher-energy electrons. The local PSD peak near $L^* \sim 4$ during this period is likely due to this contamination.

beyond $L^* \sim 6$). A positive radial gradient suggests radial transport as the acceleration mechanism: either substorm-related injections from the tail or radial diffusion from higher L. However, a more complete understanding can be had through the use of THEMIS PSD measurements for constant $\mu = 750$ MeV/G and $K < 0.01\,\mathrm{G}^{1/2}\,\mathrm{R_E}$, shown in Figure 3 (bottom). During this period, with apogee near 13 R_E, each THEMIS spacecraft cuts through the full extent of the outer belt twice every ~24 h. The THEMIS PSD gradients show a clear peak between $5 < L^* < 6$ on four consecutive passes through the outer belt between 14 January 1:35 UT and 14 January 10:27 UT. A local peak in the PSD profile such as this suggests a local acceleration mechanism occurring, such as VLF chorus. This event agrees with other recent studies that determine that PSD peaks are typically found inside of GEO [e.g., *Shprits et al.*, 2012; *Schiller et al.*, 2012; *Reeves et al.*, 2013]. Note that THEMIS PSD measurements are susceptible to high-energy electron contamination. During this period there is an enhanced high-energy electron population at $L < 5$, so the discrepancy between MagEIS PSD and THEMIS PSD in this region for this period is likely due to this contamination.

[17] Another possible cause for a peak in PSD is magnetopause shadowing [*Chen et al.*, 2007; *Turner et al.*, 2012a]. However, THEMIS PSD profiles prior to the enhancement do not show significant PSD at high L, which is required for magnetopause shadowing to be the cause of a peak in PSD. Furthermore, the magnetopause is ~9.3 R_E at the subsolar point based on *Shue et al.* [1997] magnetopause model, which would cause the PSD peak to be measured at much higher L than that observed by THEMIS.

[18] The average *Bz* for the period following the SI is negative, qualifying the event as a southward interplanetary magnetic field-dominant HSS (SBz-HSS). There are similarities between this event and the statistical result of 108 SBz-HSSs analyzed in *Miyoshi et al.* [2013] and *Miyoshi and Kataoka* [2008]. Their findings show that hot electrons (30–100 keV) provide energy for the generation of whistler waves, which in turn enhance outer radiation belt electrons. This statistical analysis provides further evidence that VLF whistler mode chorus waves are the cause of the accelerating electrons to relativistic energies.

[19] Since these measured flux and PSD values are the net result of the balance between acceleration and loss mechanisms, further analysis of low Earth orbit (LEO) precipitation measurements can provide a direct estimate on the electron precipitation rate to better quantify the magnitude, energy, and location of the acceleration mechanisms occurring during this enhancement event. To provide an estimate of loss rates, we employ CSSWE measurements and the Loss Index Method [*Selesnick*, 2006; *Tu et al.*, 2010; *Li et al.*, 2012]. This method relies on the tilt and offset of Earth's dipole magnetic field, which allows three populations to be measured by CSSWE from LEO: trapped, quasi-trapped, and untrapped. The trapped electrons are trapped in the magnetosphere beyond a drift orbit timescale, the quasi-trapped electrons are in the drift-loss cone and precipitate within a drift period, and the untrapped electrons are in the bounce-loss cone and are lost within a bounce period. Separating the different populations, under the assumption that electrons are locally mirroring if measured at the spacecraft and are lost if they reach 100 km altitude, allows the method to model pitch angle diffusion rates from CSSWE measurements and, ultimately, electron lifetimes. During the first half of 14 January (00:00 to 12:00), 0.6 MeV electrons at $L = 5.5$ had a lifetime of 10.5 days, and 1.8 MeV electrons a lifetime of 3.6 days. The mechanism that causes the observed enhancement must have consequently

accelerated 5% and 16% more electrons with energies of 0.6 MeV and 1.8 MeV, respectively, to account for atmospheric precipitation. Thus, measurements at low altitude, which are capable of resolving the loss cones, are essential to properly quantify the relative contribution between source and loss processes.

4. Summary

[20] The Van Allen Probes, THEMIS, and the CSSWE CubeSat observe a relativistic electron enhancement on 13–14 January 2013, associated with a HSS. Observations of the radiation belts during this period are unprecedented in energy resolution, radial distribution, and latitudinal coverage. This particular enhancement, which was greater than 2.5 orders of magnitude for 0.6 MeV electrons in less than 13 h, is of considerable interest due to the relatively benign geomagnetic conditions during which it occurred. Small but isolated substorm activity is present, but there is no geomagnetic storm as measured by the *Dst* index. The existence of this event, and others like it, demonstrate that large enhancements can occur independent of geomagnetic storms.

[21] The sudden, extreme enhancement (>330X in <13 h) is seen in all energy channels from ~0.6 to 1.3 MeV, but not observed at greater energies. The acceleration mechanism is estimated to be 5% and 16% larger for 0.6 MeV and 1.8 MeV electrons, respectively, than what MagEIS measurements alone indicate, due to concurrent precipitation loss into Earth's atmosphere. Radial phase space density (PSD) profiles from MagEIS observations alone do not capture the location of the PSD peak. Analysis of THEMIS PSD profiles, however, shows a local peak in PSD near $L^* \sim 5.5$, which indicates that local acceleration is the source of the relativistic electrons. Consequently, the flux enhancement observed by MagEIS is dominated by rapid inward radial transport from this peak at higher L. By using both spacecraft, we observe that the initial acceleration source of relativistic electrons is due to local heating, but the sudden and extreme flux enhancement observed by MagEIS is a direct result of a fast transport mechanism bringing relativistic electrons radially inward.

[22] Local heating, rapid radial transport, and extreme flux enhancements are commonly associated with geomagnetic activity. However, in the event described in this letter, we observe that all three processes occur during nonstorm time conditions. This event, and others like it, compels investigators to include all enhancement events in their studies, rather than relying on the assumption that storm time conditions are required for relativistic electron enhancements in the outer radiation belt.

[23] **Acknowledgments.** The authors would like to thank Allison Jaynes for helpful discussions during the writing of this article. We acknowledge J.H. King, N. Papatashvilli, and CDAWeb for the use of the geomagnetic indices. The authors are thankful for funding from NASA contracts NAS5-01072 (Van Allen Probes mission), NAS5-02099 and NNX12AJ55G (THEMIS mission), and NSF grants AGSW 0940277 (CubeSat mission) and AGS 1131869.

[24] The Editor thanks two anonymous reviewers for their assistance in evaluating this paper.

References

Angelopoulos, V. (2008), The THEMIS mission, *Space Sci. Rev.*, *141*, 5–34, doi:10.1007/s11214-008-9336-1.

Blake, J. B., et al. (2013), The Magnetic Electron Ion Spectrometer (MagEIS) instruments aboard the Radiation Belt Storm Probes (RBSP) spacecraft, *Space Sci. Rev.*, doi:10.1007/s11214-013-9991-8.

Borovsky, J. E., and M. H. Denton (2006), Differences between CME-driven storms and CIR-driven storms, *J. Geophys. Res.*, *111*, A07S08, doi:10.1029/2005JA011447.

Chen, Y., R. H. W. Friedel, and G. D. Reeves (2006), Phase space density distributions of energetic electrons in the outer radiation belt during two Geospace Environment Modeling Inner Magnetosphere/Storms selected storms, *J. Geophys. Res.*, *111*, A11S04, doi:10.1029/2006JA011703.

Chen, Y., G. D. Reeves, and R. H. W. Friedel (2007), The energization of relativistic electrons in the outer Van Allen radiation belt, *Nat. Phys.*, *3*, 614–617, doi:10.1038/nphys655.

Denton, M. H., J. E. Borovsky, R. M. Skoug, M. F. Thomsen, B. Lavraud, M. G. Henderson, R. L. McPherron, J. C. Zhang, and M. W. Liemohn (2006), Geomagnetic storms driven by ICME- and CIR-dominated solar wind, *J. Geophys. Res.*, *111*, A07S07, doi:10.1029/2005JA011436.

Dessler, A. J., and R. Karplus (1961), Some effects of diamagnetic ring currents on Van Allen radiation, *J. Geophys. Res.*, *66*, 2289.

Elkington, S. R., M. K. Hudson, and A. A. Chan (1999), Acceleration of relativistic electrons via drift resonant interactions with toroidal-mode Pc-5 ULF oscillations, *Geophys. Res. Lett.*, *26*, 3273–3276, doi:10.1029/1999GL003659.

Gonzalez, W. D., et al. (1999), Interplanetary origin of geomagnetic storms, *Space Sci. Rev.*, *88*, 529–562.

Horne, R. B., and R. M. Thorne (1998), Potential waves for relativistic electron scattering and stochastic acceleration during magnetic storms, *Geophys. Res. Lett.*, *25*(15), 3011–3014, doi:10.1029/98GL01002.

Ingraham, J. C., T. E. Cayton, R. D. Belian, R. A. Christensen, R. H. W. Friedel, M. M. Meier, G. D. Reeves, and M. Tuszewski (2001), Substorm injection of relativistic electrons to geosynchronous orbit during the great magnetic storm of March 24, 1991, *J. Geophys. Res.*, *106*, 25,759–25,776, doi:10.1029/2000JA000458.

Kim, H.-J., K. C. Kim, D.-Y. Lee, and G. Rostoker (2006), Origin of geosynchronous relativistic electron events, *J. Geophys. Res.*, *111*, A03208, doi:10.1029/2005JA011469.

Li, X., D. N. Baker, S. G. Kanekal, M. Looper, and M. Temerin (2001), SAMPEX long term observations of MeV electrons, *Geophys. Res. Lett.*, *28*, 3827.

Li, X., D. N. Baker, S. Elkington, M. Temerin, G. D. Reeves, R. D. Belian, J. B. Blake, H. J. Singer, W. Peria, and G. Parks (2003), Energetic particle injections in the inner magnetosphere as a response to an interplanetary shock, *J. Atmos. Sol. Terr. Phys.*, *65*(2), 233–244, doi:10.1016/S1364-6826(02)00286-9.

Li, X., S. Palo, R. Kohnert, D. Gerhardt, L. Blum, Q. Schiller, D. Turner, W. Tu, N. Sheiko, and C. S. Cooper (2012), Colorado student space weather experiment: Differential flux measurements of energetic particles in a highly inclined low Earth orbit, in *Dynamics of the Earth's Radiation Belts and Inner Magnetosphere*, Geophys. Monogr. Ser., vol. 199, edited by D. Summers, et al., pp. 385–404, AGU, Washington, D. C., doi:10.1029/2012GM001313.

Li, X., et al. (2013), First results from CSSWE CubeSat: Characteristics of relativistic electrons in the near-Earth environment during the October 2012 magnetic storms, *J. Geophys. Res. Space Physics*, *118*, 6489–6499, doi:10.1002/2013JA019342.

Lyons, L. R., D.-Y. Lee, R. M. Thorne, R. B. Horne, and A. J. Smith (2005), Solar wind-magnetosphere coupling leading to relativistic electron energization during high-speed streams, *J. Geophys. Res.*, *110*, A11202, doi:10.1029/2005JA011254.

Meredith, N. P., M. Cain, R. B. Horne, R. M. Thorne, D. Summers, and R. R. Anderson (2003), Evidence for chorus-driven electron acceleration to relativistic energies from a survey of geomagnetically disturbed periods, *J. Geophys. Res.*, *108*(A6), 1248, doi:10.1029/2002JA009764.

Miyoshi, Y., and R. Kataoka (2008), Flux enhancement of the outer radiation belt electrons after the arrival of stream interaction regions, *J. Geophys. Res.*, *113*, A03S09, doi:10.1029/2007JA012506.

Miyoshi, Y., R. Kataoka, Y. Kasahara, A. Kumamoto, T. Nagai, and M. F. Thomsen (2013), High-speed solar wind with southward interplanetary magnetic field causes relativistic electron flux enhancement of the outer radiation belt via enhanced condition of whistler waves, *Geophys. Res. Lett.*, *40*, 4520–4525, doi:10.1002/grl.50916.

Morley, S. K., R. H. W. Friedel, E. L. Spanswick, G. D. Reeves, J. T. Steinberg, J. Koller, T. Cayton, and E. Noveroske (2010), Dropouts of the outer electron radiation belt in response to solar wind stream interfaces: Global positioning system observations, *Proc. R. Soc. A*, *466*, doi:10.1098/rspa.2010.0078.

O'Brien, T. P., R. L. McPherron, D. Sornette, G. D. Reeves, R. Friedel, and H. J. Singer (2001), Which magnetic storms produce relativistic electrons at geosynchronous orbit?, *J. Geophys. Res.*, *106*(A8), 15,533–15,544, doi:10.1029/2001JA000052.

Reeves, G. D. (1998), Relativistic electrons and magnetic storms: 1992–1995, *Geophys. Res. Lett.*, *25*(11), 1817–1820.

Reeves, G. D., K. L. McAdams, R. H. W. Friedel, and T. P. O'Brien (2003), Acceleration and loss of relativistic electrons during geomagnetic storms, *Geophys. Res. Lett.*, *30*(10), 1529, doi:10.1029/2002GL016513.

Reeves, G. D., et al. (2013), Electron acceleration in the heart of the Van Allen radiation belts, *Science*, doi:10.1126/science.1237743.

Schiller, Q., X. Li, J. Koller, H. Godinez, and D. L. Turner (2012), A parametric study of the source rate for outer radiation belt electrons using a Kalman filter, *J. Geophys. Res.*, *117*, A09211, doi:10.1029/2012JA017779.

Selesnick, R. S. (2006), Source and loss rates of radiation belt relativistic electrons during magnetic storms, *J. Geophys. Res.*, *111*, A04210, doi:10.1029/2005JA011473.

Shprits, Y., M. Daae, and B. Ni (2012), Statistical analysis of phase space density buildups and dropouts, *J. Geophys. Res.*, *117*, A01219, doi:10.1029/2011JA016939.

Shue, J.–H., J. K. Chao, H. C. Fu, C. T. Russell, P. Song, K. K. Khurana, and H. J. Singer (1997), A new functional form to study the solar wind control of the magnetopause size and shape, *J. Geophys. Res.*, *102*(A5), 9497–9511, doi:10.1029/97JA00196.

Spence, H. E., et al. (2013), Science goals and overview of the Energetic Particle, Composition, and Thermal Plasma (ECT) suite on NASA's Radiation Belt Storm Probes (RBSP) mission, *Space Sci. Rev.*, doi:10.1007/s11214-013-0007-5.

Temerin, M., and X. Li (2002), A new model for the prediction of *Dst* on the basis of the solar wind, *J. Geophys. Res.*, *107*(A12), 1472, doi:10.1029/2001JA007532.

Temerin, M., and X. Li (2006), *Dst* model for 1995–2002, *J. Geophys. Res.*, *111*, A04221, doi:10.1029/2005JA011257.

Tsyganenko, N. A. (1989), A magnetospheric magnetic field model with a warped tail current sheet, *Planet. Space Sci.*, *37*, 5–20, doi:10.1016/0032-0633(89)90066-4.

Tu, W., R. Selesnick, X. Li, and M. Looper (2010), Quantification of the precipitation loss of radiation belt electrons observed by SAMPEX, *J. Geophys. Res.*, *115*, A07210, doi:10.1029/2009JA014949.

Tu, W., S. R. Elkington, X. Li, W. Liu, and J. Bonnell (2012), Quantifying radial diffusion coefficients of radiation belt electrons based on global MHD simulation and spacecraft measurements, *J. Geophys. Res.*, *117*, A10210, doi:10.1029/2012JA017901.

Turner, D. L., Y. Y. Shprits, M. Hartinger, and V. Angelopoulos (2012a), Explaining sudden losses of outer radiation belt electrons during geomagnetic storms, *Nat. Phys.*, *8*(3), 208–212, doi:10.1038/nphys2185.

Turner, D. L., V. Angelopoulos, Y. Shprits, A. Kellerman, P. Cruce, and D. Larson (2012b), Radial distributions of equatorial phase space density for outer radiation belt electrons, *Geophys. Res. Lett.*, *39*, L09101, doi:10.1029/2012GL051722.